Available online at www.sciencedirect.com
ScienceDirect
Journal of Power Sources 162 (2006) 1029–1035
JOURNAL OF POWER SOURCES
www.elsevier.com/locate/jpowsour

Gas distribution in molten-carbonate fuel cells

Tatsunori Okada [a,*], Shuichi Matsumoto [a], Mitsuie Matsumura [a], Masayuki Miyazaki [a], Minoru Umeda [b]

[a] *Mitsubishi Electric Corporation, Advanced Technology R&D Center, Fuel Cell Technologies Project, 8-1-1, Tukaguchi-honmachi, Amagasaki, Hygo 661-8661, Japan*
[b] *Nagaoka University of Technology, Nagaoka, Nigata 940-2188, Japan*

Received 7 March 2006; received in revised form 11 August 2006; accepted 14 August 2006
Available online 22 September 2006

Abstract

This paper presents an investigation of the gas distribution in a large-scale stack such as a 200-kW internal reforming (IR) molten-carbonate fuel cell (MCFC) stack. The gas flow scheme is important for the performance of the cell and for the temperature distribution. In order to supply gas to each cell uniformly and to achieve a reasonable temperature distribution, we have proposed a large-scale stack divided into four blocks from the point of view of the gas flow scheme. In our proposal, each block consists of 55 cells, 9 internal reforming units, and 1 internal manifold. The flow variation was examined by measurements on an element, numerical analysis, and measurements on a stack. We have found that (i) the flow variation among the four blocks is 1.5% or less and can be made better by using an orifice plate; (ii) the flow variation along the stacking direction in each block is within ±1%; (iii) improvement of the flow distribution in the reforming unit affects the uniformity of the temperature distribution in the cell area. These results can improve the prospects for 200 kW stacks.

Keywords: Flow distribution; Internal reforming; MCFC; Fuel cells; Electrochemical generation

1. Introduction

A molten-carbonate fuel cell (MCFC) is constructed from electrode plates (anode and cathode) placed in close contact with the surfaces of an electrolyte plate, and, over the surfaces of the electrode plates, an anode gas (fuel gas) and a cathode gas (oxidizing gas) flow to perform electrochemical power generation. A stack consists of several such single cells, placed between electrically conductive separator plates; anode and cathode gases are supplied to the cells through a manifold that connects the cells in the stacking direction.

On the anode side, hydrogen and carbon monoxide, used as the fuel gas, take part in the cell reaction expressed by Eqs. (1) and (2) below. These gases are generally created from natural gas or other hydrocarbons, supplied as the original fuel, using a catalyst and the reforming reaction expressed by Eq. (3) and the shift reaction expressed by Eq. (4):

$$H_2 + \tfrac{1}{2}O_2 \leftrightarrow H_2O + Q_1 \quad (1)$$

$$CO + \tfrac{1}{2}O_2 \leftrightarrow CO_2 + Q_2 \quad (2)$$

$$CH_4 + H_2O \leftrightarrow CO + 3H_2 - Q_3 \quad (3)$$

$$CO + H_2O \leftrightarrow CO_2 + H_2 + Q_4 \quad (4)$$

Since the reforming reaction takes place at 600 °C or higher, in the same temperature region as the cell reaction, flat-plate reforming units filled with a reforming catalyst may be placed in a separate area in the stack; this method is called an indirect internal reforming (IR) method. A reforming reaction can also be performed in the anode gas flow channel, filled with reforming catalyst, simultaneously with the cell reaction; this is called a direct internal reforming method. These methods can eliminate the need for an external hydrogen production unit. Both methods are called internal reforming; we refer to an MCFC that uses these methods jointly as an advanced IR-MCFC.

* Corresponding author. Tel.: +81 6 6497 7181/4 4520 5261; fax: +81 6 6497 7292/4 4520 5263.
E-mail addresses: tkyhmokada@ybb.ne.jp, okadattn@nedo.go.jp (T. Okada).

0378-7753/$ – see front matter © 2006 Elsevier B.V. All rights reserved.
doi:10.1016/j.jpowsour.2006.08.012

Nomenclature

d	Typical diameter of flow channel
f_i	Friction factor of flow channel element i
L	Length of flow channel
ΔP_i	Pressure difference across element i
Q	Enthalpy
Re	Reynolds number ($=\rho Vd/\mu$)
U_f	Utilization ratio of anode gas (the "utilization ratio" means the ratio of the quantity of gas consumed in the cell reaction to the quantity of gas supplied)
U_{ox}	Utilization ratio of cathode gas (oxygen)
V_i	Velocity of flow in element I

Greek symbols

μ	Gas viscosity
ρ	Gas density
ξ	Assumed total friction factor

The reforming reaction expressed by Eq. (3) is endothermic; the shift reaction of Eq. (4), which is exothermic, occurs simultaneously, but the excess energy is taken away by the cathode gas because of the inequality $Q_3 < Q_1 + Q_2 + Q_4$. Consequently, the temperature may decrease to lower than 550 °C, at which temperature the electrolyte would solidify, if the reforming reaction and the cell reaction were to occur intensively in different areas on the surface, permitting the possibility that the cell reaction might stop or high-temperature areas might arise that would accelerate the deterioration of structural members. Therefore, it is important to keep the gas distribution over the surface of each cell and in the stacking direction uniform and to maintain the cell reaction and reforming reaction in good balance on the surface. This is a unique challenge for high-temperature fuel cells such as MCFCs and solid-oxide fuel cells (SOFCs) that work at higher temperatures, and is different from the case of low-temperature fuel cells, such as polymer electrolyte fuel cells (PEFCs), which react at lower than 100 °C, and phosphoric acid fuel cells (PAFCs), which react at approximately 200 °C; in the case of low-temperature fuel cells, temperature control by means of cooling water supplied to each cell is relatively easy.

Recently, the development of large-scale demonstration plants has shown significant progress [1]. Commercialization programs have been reported [2,3]. Therefore, it is increasingly important for practical stacks to achieve uniformity of gas flow in each cell and in the stacking direction, and to achieve long-term uniform cell performance. Previous research [4,5] have been reported on the gas flow dynamics of MCFC stacks, however, these reports targeted external reforming type of MCFC stack, and the Reynolds number (Re) 100–800, these ranges are too high for internal reforming type of MCFC stack with high gas utilization flow to reflect actual stack. Hence, about the actual flow range of Re, we have studied the method of gas distribution for a flat-plate reforming unit consisting of layers at intervals of several cells, with channels on the cell surfaces, and with a gas feed to each cell that is uniform in the stacking direction, with the aim of realizing a uniform gas supply to an IR-MCFC stack of the 200 kW class, which may be the scale of a stack in a power plant.

2. Gas distribution in flat-plate reforming unit

A flat-plate reforming unit, when used in an indirect reforming scheme in a front stage containing one unit for every six cells, reforms approximately 80% of the fuel before it enters the cell. Therefore, any variation over the surface of the reforming unit may greatly affect the temperature distribution over the cell surface, and the temperature may, in some cases, become lower than 550 °C, at which the molten-carbonate electrolyte solidifies. In the past, the present authors have studied the optimization of the flow direction in the reforming unit, and the temperature distribution in it [6,7]. In the current study, we deal with the effect of the gas distribution on the temperature distribution inside a reforming unit [8].

The reforming unit used in our study consisted of flat plates with an external size of 1700 mm × 900 mm and a thickness of approximately 10 mm. Fig. 1 shows the relationship between the fuel gas flow in the reforming unit and the flow of anode and cathode gases in the cell area. Table 1 shows the Reynolds number and several parameter of each flow element. The fuel is supplied from the side, its flow direction turns by 90° in the distribution section, and the gas then reaches the catalyst-filled layer. It is required that the gas should be distributed uniformly over the width of the flow channel and that the pressure should also be distributed uniformly. To meet this requirement, in this study we have used corrugated plates in the channel and the reinforcing materials, and varied the width of the flow channel upstream of the distribution section, for several types of reforming unit and using several different velocities and pressures. We determined the distribution of the flow velocity from a convergence calculation by splitting the unit into 10 meshes across its width under the condition that the differential pressure should be constant from the branch pipe to the flow joint. Further, as a trial, we made two typical reforming units and examined the

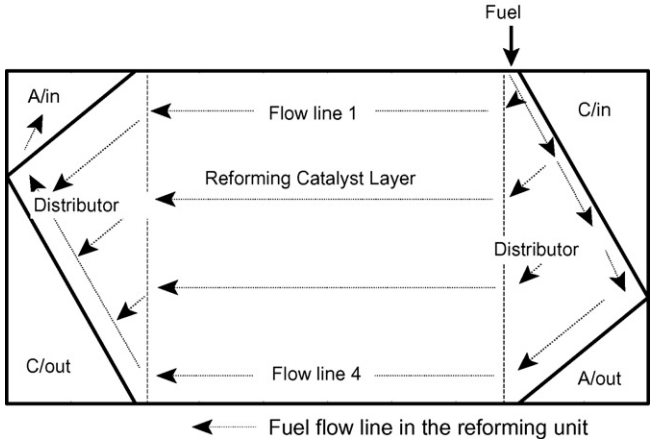

Fig. 1. Fuel flow pattern in a reforming unit.

Table 1
Several properties of anode flow element

Element	Diameter, d (m)	Gas density, ρ (kg m^{-3})	Viscosity, μ (kg s^{-1} m^{-1})	Inlet average velocity, V (m s^{-1})	Reynolds number, Re
Fuel-feeding port	1.00E−02	0.245	2.96E−05	63.8	5280
Upstream of the distributor[a]					
Unit A	2.00E−02			16.0	2650
Unit B	1.33E−02			36.1	3970
Reforming catalyst layer[b]	2.95E−3[c]			0.81	19.8

[a] Before flow direction turn by 90°.
[b] Corrugated plates of three laminated and no catalyst.
[c] Corrugated pitch and depth.

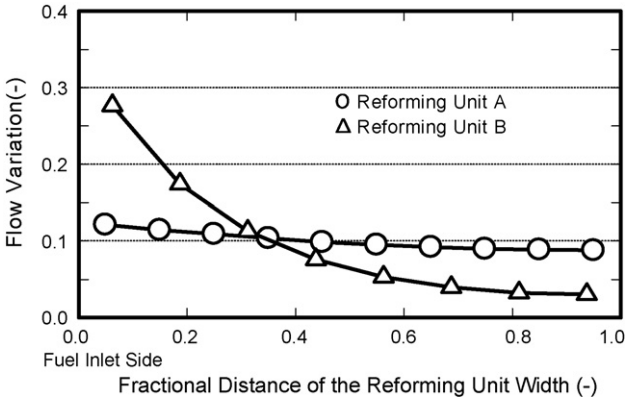

Fig. 2. Calculated flow variation in reforming units A and B.

actual temperature distribution on the basis of the result of a stack test.

Fig. 2 shows the distribution of the flow velocity at the inlet of the catalyst layer, determined by a numerical calculation, for two types of reforming units, namely reforming unit A, which had the smallest drift, and reforming unit B, which had the greatest drift. The results reveal that an almost uniform flow is secured in reforming unit A, but in reforming unit B, approximately 80% of the gas fed in flows only in half of the area of the fuel-feeding port. Figs. 3 and 4 show the temperature distribution

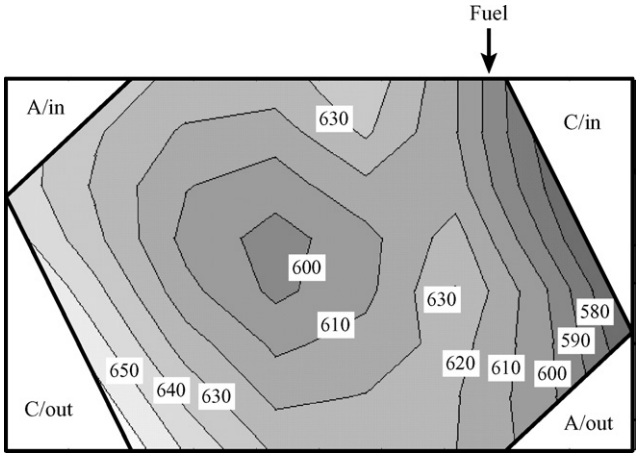

Fig. 3. Calculated temperature distribution in the cell area adjoining a reforming unit (uniform flow in reforming unit).

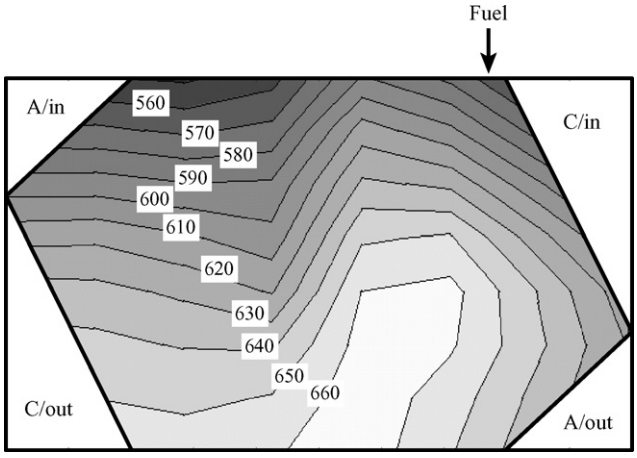

Fig. 4. Calculated temperature distribution in the cell area adjoining a reforming unit (drift of flow in reforming unit).

in the cell area adjoining the reforming unit in stacks in which units of type A and B, respectively, were installed. These contour maps indicate that the temperature increases gradually from the cathode entry side (C/in) in reforming unit A, but around the central area, the temperature on the cathode outlet side (C/out) is maintained at 650 °C, cooled by the reforming reaction. In reforming unit B, the distribution of the endothermic reaction is concentrated on the side where flow line 1 (see Fig. 1) is, permitting a region where the temperature is 560 °C or lower along the flow channel on the side where the fuel-feeding port is located. It may be conjectured that this is due to the drift found in the reforming unit or, in other words, because the rate of flow around flow line 1 is greater than the rate around flow line 4.

On the basis of the results above, we chose to build experimentally a tall stack that adopted the structure of reforming unit A so that a satisfactory temperature distribution might be expected.

3. Distribution of gas to cells in the stack direction

Fig. 5 shows the laminated structure of an IR-MCFC stack and the gas flow in the stack. The anode gas is supplied from an external manifold on the side wall of the stack to a flat-plate reforming unit, which consist of a front-stage reforming section at intervals of six cells; after the reforming reaction, the gas is distributed and supplied to the cell surfaces from the manifold

Table 2
Several properties in the manifold and cell area

Element	Diameter, d (m)	Gas density, ρ (kg m^{-3})	Viscosity, μ (kg s^{-1} m^{-1})	Average velocity, V (m s^{-1})	Reynolds number, Re
Anode side					
Middle manifold[a]	1.70E−01	0.165	3.09E−05	14.00	12709
Gas channel (cell area)	2.95E−03			1.55	24
Cathode side					
Inlet manifold[a]	3.20E−01	0.406	3.87E−05	18.1	60800
Gas channel (cell area)	2.95E−03			2.90	89

[a] 200 cells stack.

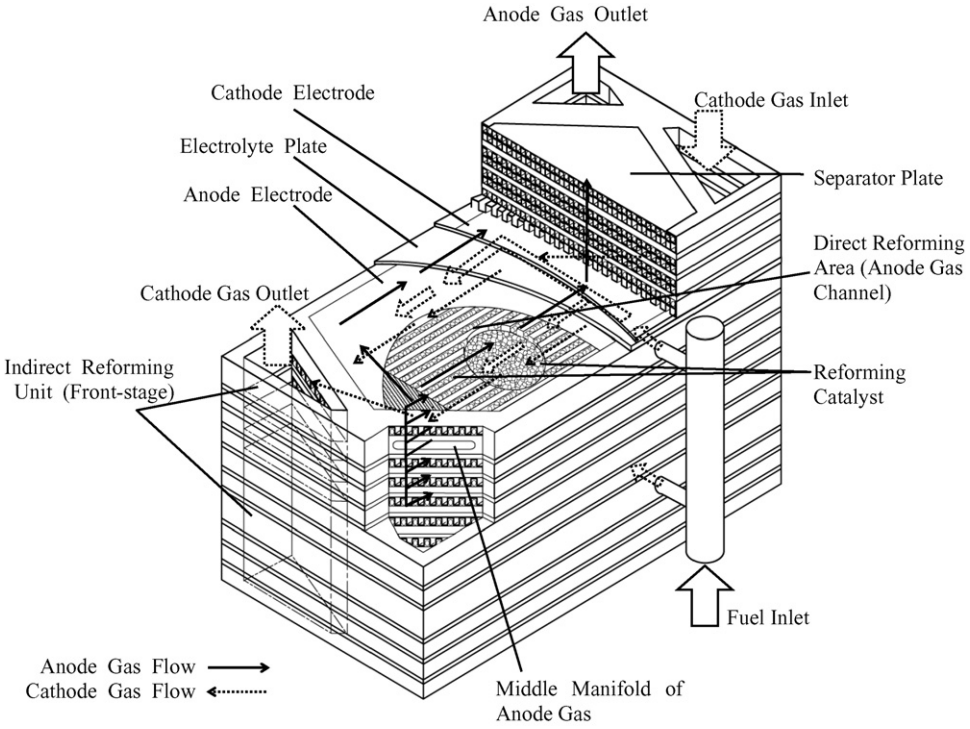

Fig. 5. Model of gas flow in IR-MCFC stack, and cutaway view.

at a corner of the cell, as shown in Fig. 1. The gas is then exhausted from the anode gas outlet manifold after hydrogen has been consumed in the cell reaction. The cathode gas is supplied to each cell from the cathode gas inlet manifold in which flow is turbulent in case of 200 cells stack, at another corner of the cell, and is then exhausted from the cathode gas outlet manifold located on the opposite corner. In the cell area and in the front-stage reforming section, the cathode gas flows parallel to the fuel gas in the front-stage reforming section; it flows in the direction opposite to the flow in the anode gas channel, which constitutes the back-stage reforming section. Table 2 shows the Reynolds number and other parameters of anode and cathode gas in manifold and cell area.

Fig. 6 shows the flow distribution when the gases were supplied at the rated flow rate; here, nine units of the front-stage reforming section were used, one for every six cells in the stack direction. This figure indicates that the variation in the flow rate is about ±2.5%, and thus the target for the flow rate distribution in the stack direction, namely ±3%, has been achieved. This target

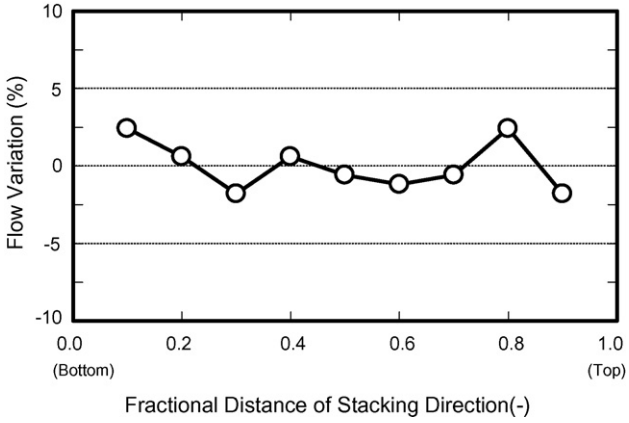

Fig. 6. Flow distribution in stacking direction in the inlet manifold of a reforming unit.

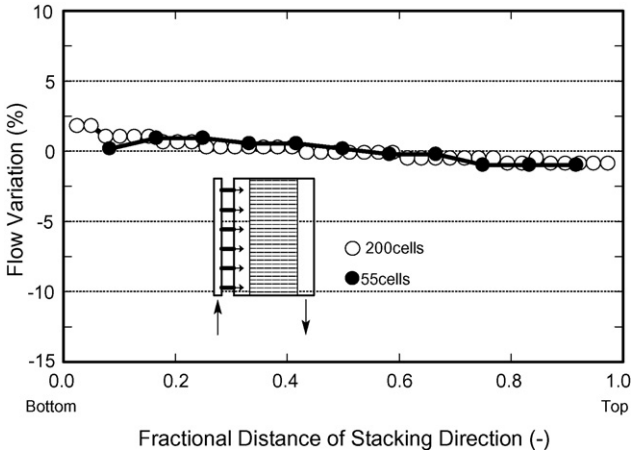

Fig. 7. Variation of anode gas flow in stacking direction.

was set as a result of considering the amounts of heat absorbed and emitted and the cell voltage. Subsequently, we measured the drift in the stack direction on the anode and cathode sides using a full-size dummy stack made of resin having an area of 1 m^2; this was done for two cases, with 55 and 200 cells in the stack. Measurement results are plotted in Fig. 7 for the anode side and Fig. 8 for the cathode side. The measurements were conducted at room temperature, and the gas supplied was air, of which quantity was approximately 1.4 $m^3\ s^{-1}$ for cathode side and 0.3 $m^3\ s^{-1}$ for anode side in the case of 200 cells. The quantity of gas supplied was selected so that the Reynolds number would be the same as that indicated in Table 2. The static pressure on the internal wall of the manifold was measured along the stack direction, and the mean flow velocity in the cell flow channel was determined from the differential pressure between the inlet and outlet manifolds using the following Eq. (5) [9], if the friction factor f_i is used Hargen-Poiseuille equation due to laminar flow in the gas channel.

$$\Delta P_i = \frac{1}{2} f_i \rho V_i^2 \left(\frac{L}{d}\right) \tag{5}$$

Figs. 7 and 8 show the measurement data in the case of Table 2 conditions. These figures indicate that the trend in the flow velocity in the stacks is such that on the anode side the velocity is larger at the bottom, while on the cathode side the velocity is larger at the top; that is, the anode and cathode sides show different patterns [10]. The reason for this seems to be because the gas is supplied uniformly into the manifold from the reforming unit, in which elements are mounted at six-cell intervals, preventing a static pressure distribution building up on the anode inlet side, whereas in the bottom area near to the outlet piping on the outlet side, the static pressure becomes lower owing to the increased velocity of flow, and thus the pressure difference between the inlet and the outlet is greater on the lower side. On the cathode side, the outlet side has a static pressure distribution similar to that on the anode side, but on the inlet side, the static pressure loss at the bottom due to the blowing-in from the piping is greater than on the outlet side, and therefore the differential pressure between the inlet and the outlet in the stack direction is smaller at the bottom. In the case of 200 cells, blow-in velocity is 46.6 m s^{-1}, velocity pressure drop $(1/2)\rho V_i^2$ is 441 Pa. This value is large compared with average channel pressure drop as approximately 1300 Pa. But blow-in velocity is decreased suddenly to 66 Pa into the manifold. In the case of 55 cells, it is easily found that the influence of blow-in velocity is small. Therefore, it is thought that difference result from reference [1] is caused by this reason.

The amount of drift is about ±1%, both on the anode side and on the cathode side, for 55 cells, which is not significant enough to affect cell performance. For 200 cells, the drift is found to be ±3% on the anode side and ±5% on the cathode side; the latter value is far off the above-mentioned target value.

4. Distribution of gas to blocks

Following the result of the investigation of drift in the stack direction described in the previous section, we considered a stack divided into four blocks in the stack direction, with 55 cells placed in each block. Fig. 9 shows a schematic piping system. The cathode gas flows through branches from the main inlet pipe and is distributed to the cells from the end plate at the top of each block, passing through a manifold located inside. After contributing to the cell reaction in the cells, the gas flows through more branch pipes to be gathered in the main outlet pipe, and then exits the branch system.

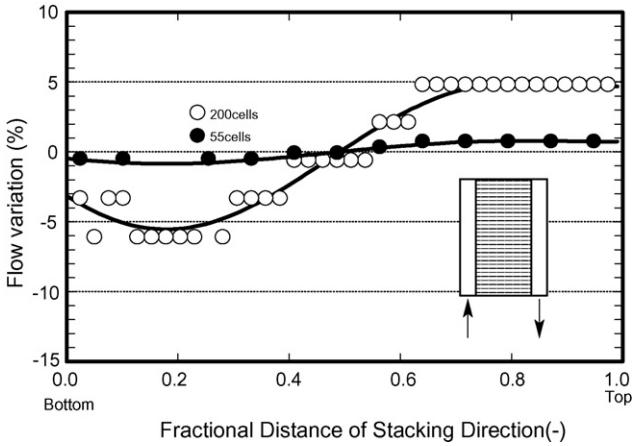

Fig. 8. Variation of cathode gas flow in stacking direction.

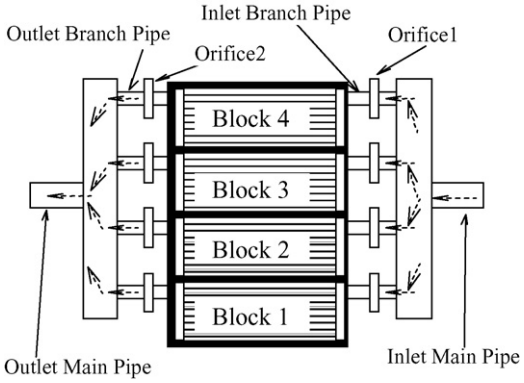

Fig. 9. Layout of flow in multi-block stack.

Table 3
Measurement conditions and specifications

Gas	Air
Temperature and pressure	Ambient
Flow rate	U_{ox} = 18% flow
Measurement method	ΔP in orifice 2
Diameter (branch pipe/orifice 1/orifice 2)	208/175/92 mm
Flow resistance of orifice 1/orifice 2	ξ = 0.25/2.20

Assuming that the temperature of the piping is uniform among the blocks, the variation in the gas flow arises from differences in the pressure loss due to the different lengths of the duct lines to the blocks and differences in the elements of the resistance in the branches.

For the above configuration, the differential pressure ΔP_n between the branch from the main inlet pipe and the confluence with the main outlet pipe can be expressed by means of Eqs. (6) and (7) below. Intending to examine the relative flow rate balance here, however, we calculated ratios of flow rates between blocks using Eq. (8), on the basis of data measured in an actual-size duct network that simulated the header and blocks 1 and 2, using a flow meter of the same size as orifice 2 in Fig. 9:

$$\Delta P_1 = \Delta P_2 = \Delta P_3 = \Delta P_4 \tag{6}$$

$$\Delta P_n = \sum \tfrac{1}{2} f_i \rho V_i^2 \tag{7}$$

$$\Delta P_i = \tfrac{1}{2} \xi \rho V_i^2 \tag{8}$$

The measurement conditions are listed in Table 3. Our study focused on the conditions on the cathode side. Fig. 10 shows a plot of the measurements. This plot indicates that the value of the flow rate is smaller by about 1 or 2% in block 1 for almost the entire range of quantity of gas supplied, if the flow rate is not adjusted by means of orifice 1. Consequently, we inserted an adjustable orifice to ensure optimization. More specifically, we calculated the orifice resistance from the differential pressure ΔP that corresponded to the flow rate difference in order to determine the internal diameter. From Eq. (8), $\rho = 0.400\ \mathrm{kg\ m^{-3}}$, $V = 22.74\ \mathrm{m\ s^{-1}}$ as calculated, difference between blocks 1 and 2 $\Delta P_1 - \Delta P_2 = 26.4$ Pa as measured. Therefore, orifice inner diameter is able to calculated by using $\xi = f(d_1/d_2)$ and reference [9].

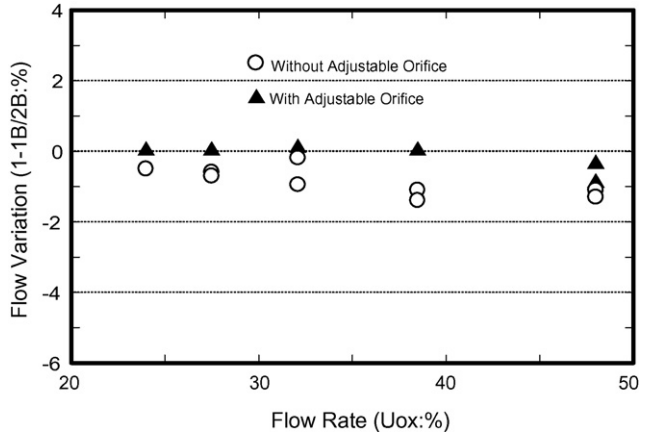

Fig. 10. Differential flow rate between blocks 1 and 2 with and without adjustable orifice.

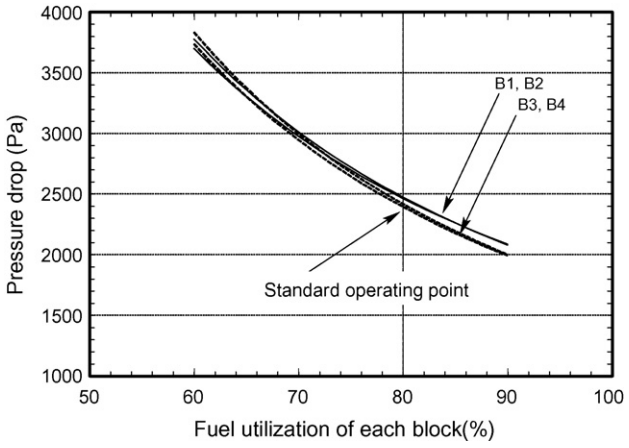

Fig. 11. Assumed pressure drop in each block vs. fuel utilization.

On the basis of the above calculation, we added an adjustable orifice 1, having an internal diameter of 84.6% of the blanch pipe to the piping of block 2, and achieved a nearly uniform distribution as shown in Fig. 10.

Similar consideration was given to the anode side, where we added an adjustable orifice 1, having an internal diameter of 87.7% of the blanch pipe to block 2. The correlation between the pressure loss and the flow rate after adjustment of the orifice resistance was applied to the operating conditions of some actual equipment in order to determine the correlation between the pressure loss and the gas utilization ratio for each block. The results, shown in Figs. 11 and 12, indicate that broadly the same pressure loss occurs under standard operating conditions in each block, on both the anode and the cathode side.

To verify the above result, we calculated the quantity of fuel supplied to each block during operation of a 200 kW stack from the composition of the outlet gas on the anode side. The result of the calculation enabled us to control the variation between blocks to within a range of ±1.0%.

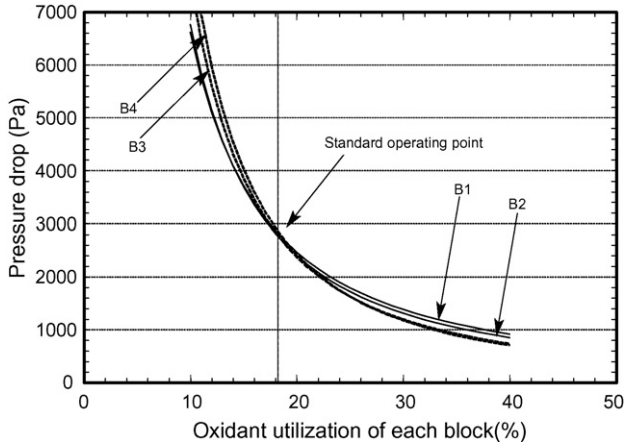

Fig. 12. Assumed pressure drop in each block vs. oxidant utilization.

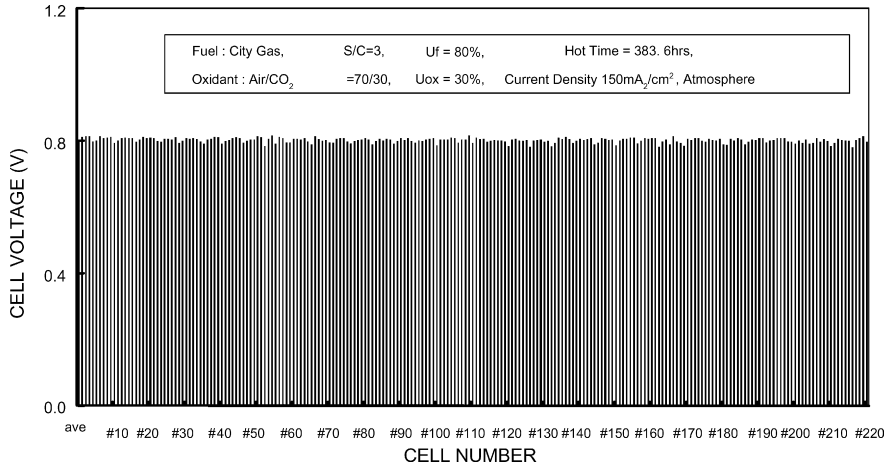

Fig. 13. Performance of each cell in a 200 kW stack.

5. Tall stack

As shown in Fig. 9, the tall stack that we considered consists of 220 cells arranged in four blocks, with 55 cells of area 1 m^2 in each block. Fig. 13 shows the values of the cell voltages when the stack was operated under standard conditions. With little difference in performance being seen between blocks, and the 220 cells showing even performance, the flow in the elements can be considered to be smooth.

6. Conclusions

With the aim of securing a uniform gas distribution in internal reforming molten-carbonate fuel cell stacks, especially large-scale and 200-kW class stacks, we have studied the drift in critical locations by means of measurements on elements in an actual piece of equipment consisting of 220 cells, by numerical analysis, and by measurements on a stack. We have proposed a tall stack separated into four blocks, where each block consists of 55 cells, 9 internal reforming units, and 1 internal manifold. The results provided us with the following findings:

(i) An excellent temperature distribution over the cell area was achieved by smoothing the flow in the reforming unit and by effective utilization of the cooling effect of the reforming reaction.
(ii) The drift between cells in a block can be controlled to 1% or less by using a configuration with 55 cells in a block.
(iii) The drift between blocks that occurs for structural reasons can be limited to 1 or 2% by adjustment of orifices.

Acknowledgement

This work was done under a contract from NEDO (New Energy and Industrial Technology Development Organization, Japan).

References

[1] Y. Izaki, H. Yasue, 2000 Fuel Cell Seminar, Portland, 2000, pp. 460–463.
[2] C. Bentley, M. Farooque, H. Maru, J. Leitman, 2000 Fuel Cell Seminar, Portland, 2000, pp. 456–459.
[3] H. Nock, J. Leitman, H. Maru, 2003 Fuel Cell Seminar, Miami Beach, 2003, pp. 945–948.
[4] N. Ono, R. Oshima, H. Koyano, Y. Sato, S. Takashima, Trans. Jpn. Soc. Mech. Eng., Ser. B 61 (581) (1995) 150–156.
[5] N. Ono, R. Oshima, H. Koyano, Y. Sato, S. Takashima, Trans. Jpn. Soc. Mech. Eng., Ser. B 61 (585) (1995) 18–23.
[6] T. Okada, H. Ide, M. Miyazaki, T. Tanaka, S. Narita, J. Ohtsuki, Proceedings of the 25th IECEC, vol. 3, Reno, 1990, pp. 207–212.
[7] T. Okada, H. Ide, M. Miyazaki, E. Nishiyama, A. Hijikata, J. Ohtsuki, Trans. Jpn. Soc. Mech. Eng., Ser. B Jpn. 58 (554) (1992) 243–248.
[8] T. Okada, M. Matsumura, A. Sasaki, Proceedings of the Sixth National Symposium on Power and Energy Systems, Japan, 1998, pp. 265–268.
[9] Japan Society of Mechanical Engineers, JSME Data Handbook: Hydraulic Losses in Pipes and Ducts, JSME, Japan, 1979, pp. 53–54.
[10] T. Okada, M. Matsumura, Proceedings of the 16th Conference on Energy and Resources, Japan, 1997, pp. 297–302.